RBM ONLINE

ELSEVIER

Article

Gene expression changes in uterine myomas in response to ulipristal acetate treatment

Guillaume E Courtoy [a], ***Jacques Donnez*** [b], ***Jérôme Ambroise*** [c], ***Pablo Arriagada*** [d], ***Mathieu Luyckx*** [e], ***Etienne Marbaix*** [f,g], ***Marie-Madeleine Dolmans*** [a,e,*]

[a] *Pôle de Recherche en Gynécologie, Institut de Recherche Expérimentale et Clinique, Université Catholique de Louvain, Avenue Mounier 52, B1.52.02, 1200 Brussels, Belgium*

[b] *Société de Recherche pour l Infertilité SRI, Avenue Grandchamp 143, 1150 Brussels, Belgium*

[c] *Center for Applied Molecular Technologies, Institut de Recherche Expérimentale et Clinique, Université Catholique de Louvain, Avenue Hippocrate 55, B1.54.01, 1200 Brussels, Belgium*

[d] *Gedeon Richter/PregLem S.A., Route de Frontenex 41A, 1207 Geneva, Switzerland*

[e] *Gynecology and Andrology Department, Cliniques Universitaires St-Luc, Avenue Hippocrate 10, 1200 Brussels, Belgium*

[f] *Pathology Department, Cliniques Universitaires St-Luc, Avenue Hippocrate 10, 1200 Brussels, Belgium*

[g] *Cell Biology Unit, de Duve Institute, Université Catholique de Louvain, Avenue Hippocrate 75, B1.75.10, 1200 Brussels, Belgium*

Guillaume E. Courtoy obtained his MSc in Biomedical Sciences from the Université Catholique de Louvain (UCL, Belgium). He is completing his PhD and currently working as a researcher at the Laboratory of Gynecology (UCL, Belgium). The topics of his PhD thesis are selective progesterone receptor modulators and uterine fibroids.

KEY MESSAGE

Ulipristal acetate significantly modifies expression of apoptosis- and extracellular-matrix-related genes in uterine myomas. Gene expression patterns differ between myomas responsive or not to this treatment. The present study constitutes the first molecular analysis of possible mechanisms to explain myoma response to ulipristal acetate treatment.

A B S T R A C T

Research question: Does ulipristal acetate (UPA) modify the expression of genes related to apoptosis or the extracellular matrix in uterine myomas and are any modifications associated with a clinical response?

Design: Targeted analysis of 176 apoptosis- or extracellular-matrix-related genes was conducted using polymerase chain reaction (PCR) arrays. Relevant results were validated by quantitative PCR. Four groups were established: responsive short-term (one course, *n* = 9), responsive long-term (two to four courses, *n* = 9), non-responsive (*n* = 9), and the control group who was not given any hormone therapy (*n* = 9). The clinical response was monitored by medical imagery and considered significant when volume reduction was greater than 25%.

* Corresponding author.
E-mail address: marie-madeleine.dolmans@uclouvain.be (M-M Dolmans).

https://doi.org/10.1016/j.rbmo.2018.04.050

Results: Compared with untreated myomas, significant changes in expression of four genes were found in UPA-treated myomas. Gene expression of *integrin subunit beta 4* was repressed by UPA treatment (fold change [FC] = –12.50, $P < 0.001$, $q < 0.001$), *tenascin-C* expression was downregulated in UPA-responsive patients (FC = –2.50, $P = 0.010$, $q = 0.090$), *survivin* was repressed in short-term UPA-responsive tumours (FC = –7.69, $P < 0.001$, $q = 0.010$), and *catenin delta 2* gene expression was upregulated in non-responsive myomas (FC = +7.36, $P < 0.001$, $q = 0.010$).
Conclusion: This characterization provides the first molecular distinction between myomas responsive or non-responsive to UPA treatment.

Introduction

Uterine myomas are the most common benign tumours found in the female reproductive tract. Depending on myoma number, volume and localization in the uterus, they can be responsible for abnormal uterine bleeding, pelvic pain and infertility (Donnez and Dolmans, 2016; Stewart, 2015). The pathogenesis is unclear and their cause is still a matter of debate. Several lines of evidence have indicated a clonal origin (Commandeur et al., 2015; Mehine et al., 2014), but no single genetic cause has yet been identified.

Recent sequencing studies, however, have revealed that uterine myomas can be divided into subclasses based on their molecular genetic background (Kampjarvi et al., 2014; Mehine et al., 2013, 2016; Yatsenko et al., 2017). Most myomas (about 70%) have mediator complex subunit 12 (*MED12*) mutations in exon 2, others overexpress high-mobility group AT-hook 2 (*HMGA2*), whereas a third group is characterized by biallelic fumarate hydratase inactivation (Mehine et al., 2014, 2016). Interestingly, these three alterations are mutually exclusive, and each subclass possesses a unique global gene expression pattern. Hence, distinct subgroups of myomas with different transcriptomic profiles may coexist (Mehine et al., 2016).

Because myoma growth depends on progesterone (Ishikawa et al., 2010; Kim and Sefton, 2012), ulipristal acetate (UPA), a selective progesterone receptor modulator (SPRM), was clinically investigated for myoma management. A single 3-month course of treatment with UPA 5 or 10 mg/day typically reduces tumour volume by 35% (Donnez *et al.*, 2012a, 2012b), and this reduction can be improved to 50% after repeated courses of treatment (Donnez *et al.*, 2014, 2016) with eventual complete disappearance (Donnez and Dolmans, 2016; Luyckx et al., 2016). In 20% of cases, myomas do not shrink or even continue to grow (Donnez et al., 2015).

We previously reported that UPA inhibits proliferation, induces apoptosis and effectively reduces extracellular matrix (ECM) content under the influence of matrix metalloproteinases (MMP) (Courtoy et al., 2015). Nevertheless, questions on how UPA mediates these mechanisms, whether they are involved in shrinkage and why some myomas do not shrink at all remain unanswered. The aim of the present study was to identify whether differences in apoptosis or ECM-related gene expression could be responsible for the response or lack of response of myomas to UPA treatment.

Materials and methods

Patients

Thirty-six patients with symptomatic uterine myomas but free of any hormone therapy for at least 3 months before inclusion were selected to undergo quantitative polymerase chain reaction (qPCR) arrays. Twenty-seven were given daily preoperative treatment with 5 mg or 10 mg UPA either one 3-month course (considered short-term), or two to four 3-month courses (considered long-term) in the context of two clinical studies (Donnez *et al.*, 2014, 2016). The volume of each myoma was monitored by magnetic resonance imaging or ultrasound as part of the clinical management, and calculated using the formula $4/3.\pi.r_1.r_2.r_3$. in mm^3 (where r_1, r_2 and r_3 represent the radii in the three dimensions). A significant response to treatment was defined as at least a 25% reduction in volume, as this threshold is clinically relevant (Donnez *et al.*, 2014). Three treatment groups were then established: responsive to short-term (ST) treatment, long-term (LT) treatment, and non-responsive (NR), with no distinction between short- or long-term treatment. The control group included the remaining nine women with symptomatic myomas who did not receive any treatment. All patients underwent myomectomy or hysterectomy. Population characteristics (including race, age, BMI, end of treatment to surgery (wash-out) time, myoma volume before and after treatment) are detailed in Supplementary Table S1. Use of human tissues was approved by the Institutional Review Board of the Université Catholique de Louvain, Brussels (IRB 2015/19OCT/556).

Tissue samples

Fresh myoma samples were collected directly from the operating room to ensure that the total time between clamping of the vessels and complete tissue sampling never exceeded 45 min. Biopsies were dissected into 2-mm^3 pieces and immediately frozen in TRIzol reagent (Thermo Fisher Scientific, Merelbeke, Belgium) for RNA extraction and stored at –80°C.

RNA extraction

Total RNA extraction was carried out using TRIzol reagent (Thermo Fisher Scientific) according to the manufacturer's protocol, as previously described (Van Langendonckt et al., 2014). Purified RNA concentrations were determined in all samples using a microvolume spectrophotometer (NanoDrop ND1000, Thermo Fisher Scientific), and purity was determined by $A_{260/280}$ ratios >1.90. RNA quality was assessed using an Agilent 2100 Bioanalyzer automated analysis system (Agilent Technologies, Santa Clara, CA, USA) with proprietary total eukaryotic RNA 6000 nano chiplet. Only samples with an RNA integrity number of seven or over and no traces of genomic DNA were analysed further by PCR. Extracted RNA remained at –80°C until reverse transcription.

Reverse transcription

Total RNA (3.0 µg) was reverse transcribed with random hexamers (1.25 mM, Thermo Fisher Scientific), dNTP (2 mM, Thermo Fisher Scientific), RNasin (20 U, Thermo Fisher Scientific) and SuperScript® III reverse transcriptase (100 U, Thermo Fisher Scientific) in a final volume

of 20.0 µl. The amplification protocol included preliminary incubation for 5 min at 24°C, followed by 1 h at 55°C to allow reverse transcription activity, before inactivation for 15 min at 70°C. Synthesized cDNA was stored at –20°C until use.

Quantitative PCR arrays

The TaqMan gene expression array method was chosen as it is highly quantitative, allows normalization with multiple internal control genes (Vandesompele et al., 2002) and shows high reproducibility and good sensitivity thanks to multiple transcript detection (Dallas et al., 2005). Commercial human ECM and adhesion molecules and human apoptosis PCR arrays (Thermo Fisher Scientific) were selected because they include probes for previously identified candidate genes. Details of the different genes and probes used in these PCR arrays are presented in Supplementary Table S2 and Supplementary Table S3. Five samples per group (totalling 20) were analysed once by each of the two PCR arrays, according to the manufacturer's protocol. Briefly, amplification was carried out with 25.0 ng cDNA per well with the TaqMan Universal PCR Master Mix (Thermo Fisher Scientific) in a final volume of 20.0 µl. Thermal cycling conditions involved an initial step for cDNA denaturation and hot-start polymerase activation for 2 min at 50°C, then 10 min at 95°C, followed by cDNA amplification with 45 cycles of 30 s at 95°C and 1 min at 60°C using the Mx3005P qPCR System (Agilent) for FAM™ and ROX™ detection. Threshold cycle (CT) values were exported from proprietary software MxPro v4.10 (Agilent) to be analysed on R software (www.r-project.org).

Quantitative PCR on additional myoma samples

Polymerase chain reaction arrays identified gene transcripts with significant changes in expression levels differentially expressed according to treatment, and with a known and relevant biological function in apoptotic and ECM remodelling processes. On the basis of these criteria, 11 candidate genes were further investigated on four additional myoma samples per group by real-time qPCR using the same TaqMan gene expression probes as for PCR arrays (Thermo Fisher Scientific). Because the first experiment determined the *HPRT1* gene to be the best reference gene, it was selected for endogenous RNA controls for this study extension. Polymerase chain reactions were carried out in duplicate in the same conditions as PCR arrays, and negative controls (no RNA template control, no reverse transcriptase control and no DNA polymerase control) were included. No replicates showed a variation of more than 0.5 threshold cycles in the real-time qPCR experiments, with most exhibiting less than 0.2 threshold cycles of variation. Threshold cycle values were calculated from replicates with proprietary software (MxPro v4.10, Agilent) and exported for statistical analysis using R software. Data on the 11 candidate genes plus the best housekeeping gene (HKG) as determined by PCR arrays, were added to the results of the PCR arrays to increase the power of the analysis (final $n = 9$ per group).

Analysis of quantitative PCR arrays and quantitative PCR extension

All transcriptomic data were analysed on R software. In a first step, all 'non-detect' values were processed using the R package for non-detects (v2.6.0). It has indeed been reported that the common practice of setting non-detect values equal to 40 introduces substantial bias in differential expression (McCall et al., 2014). In this R package, it is assumed that missing data represent a true threshold cycle value over 40; a completely unexpressed transcript; or failure to detect a true threshold cycle value less than 40. Missing data are therefore imputed using an algorithm based on an expectation–maximization approach.

In a second step, the stability of 12 HKG was tested using geNorm on the principle that ideal reference genes should be similarly expressed regardless of treatment conditions. The software detected threshold cycle variations for each of the reference genes across the samples. Genes showing the greatest expression variability among the 12 HKG tested were iteratively excluded, until only the most stable HKGs remained (Dupasquier et al., 2014) (Supplementary Table S4). Expression stability (*M*-value) was calculated as described (Vandesompele et al., 2002). Expression levels of each gene were then normalized according to the selected HKGs by computing ΔCT values. The Limma package (Bioconductor v3.26.9) was used to determine ΔΔCT values and associated *P*-values of each gene in the four groups (Smyth, 2005). Fold change (FC) differences were determined as $2^{-(\Delta CT\ sample\ -\ \Delta CT\ control)}$. $P < 0.05$ was considered statistically significant. Because a large panel of genes was simultaneously assessed and multiple comparisons were carried out, *P*-values were adjusted for multiple testing using the Benjamini–Hochberg method, and $Q < 0.100$ was considered significant to account for a 10% false discovery rate.

Results

Targeted transcriptomic analysis by quantitative PCR arrays

Total RNA from five untreated (CTL), five short-term-treated UPA-responsive, five long-term-treated UPA-responsive, and five UPA-non-responsive myomas was analysed by apoptosis and ECM-related gene expression arrays.

Determining the best housekeeping genes

First, 12 commonly used HKGs present on ECM arrays were compared to determine the best reference genes. The robustness of each HKG was evaluated by measuring its respective expression stability (*M*-value). *HPRT1* was found to be particularly stable ($M = 0.448$) (Supplementary Table S4), compared with the commonly referenced *18S*, *ACTB*, *B2M* and *GAPDH* genes. Among the tested HKGs, *HPRT1*, *PGK1* and *PPIA* were identified as the most stable, and were therefore selected for normalization.

Extracellular matrix-related genes differentially expressed after ulipristal acetate treatment

Of the 84 candidate genes related to the ECM, the most highly expressed genes were found coding for ECM structural proteins like collagens and fibronectin (**Figure 1**), but no significant change in gene expression levels was noted between the four groups. The 11th most abundant gene transcribed in the control group (*TNC*) showed a tendency towards repression in the UPA-treated groups compared with the control group (ST: FC = –2.78, $P = 0.030$; LT: FC = –3.13, $P = 0.018$; NR: FC = –2.94, $P = 0.023$. No difference remained significant after statistical adjustment, $Q > 0.100$).

Some factors involved in ECM remodelling made up the second group of the most highly expressed genes (*TIMP2*, *MMP2*, *TIMP1*, *TIMP3*), with no difference in expression levels between groups. Notably, *MMP2* expression was similar throughout (**Figure 1**), whereas

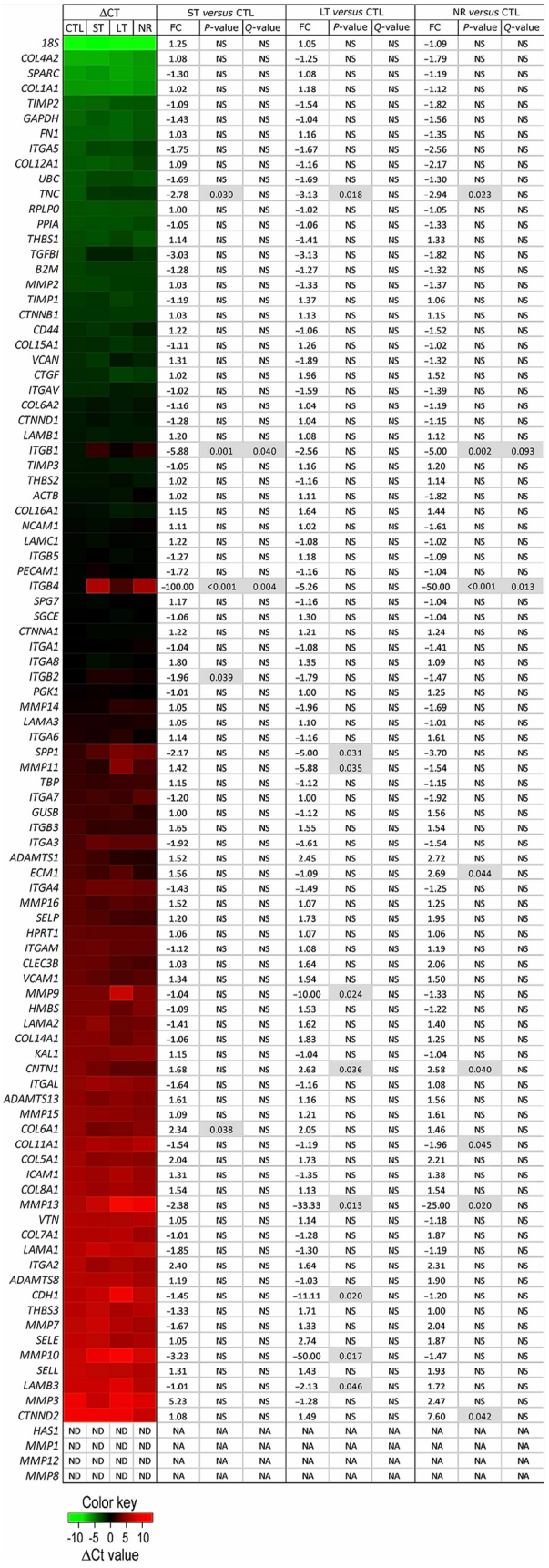

	ΔCT				ST *versus* CTL			LT *versus* CTL			NR *versus* CTL		
	CTL	ST	LT	NR	FC	*P*-value	Q-value	FC	*P*-value	Q-value	FC	*P*-value	Q-value
18S					1.25	NS	NS	1.05	NS	NS	−1.09	NS	NS
COL4A2					1.08	NS	NS	−1.25	NS	NS	−1.79	NS	NS
SPARC					−1.30	NS	NS	1.08	NS	NS	−1.19	NS	NS
COL1A1					1.02	NS	NS	1.18	NS	NS	−1.12	NS	NS
TIMP2					−1.09	NS	NS	−1.54	NS	NS	−1.82	NS	NS
GAPDH					−1.43	NS	NS	−1.04	NS	NS	−1.56	NS	NS
FN1					1.03	NS	NS	1.16	NS	NS	−1.35	NS	NS
ITGA5					−1.75	NS	NS	−1.67	NS	NS	−2.56	NS	NS
COL12A1					1.09	NS	NS	−1.16	NS	NS	−2.17	NS	NS
UBC					−1.69	NS	NS	−1.69	NS	NS	−1.30	NS	NS
TNC					−2.78	0.030	NS	−3.13	0.018	NS	−2.94	0.023	NS
RPLP0					1.00	NS	NS	−1.02	NS	NS	−1.05	NS	NS
PPIA					−1.05	NS	NS	−1.06	NS	NS	−1.33	NS	NS
THBS1					1.14	NS	NS	−1.41	NS	NS	1.33	NS	NS
TGFBI					−3.03	NS	NS	−3.13	NS	NS	−1.82	NS	NS
B2M					−1.28	NS	NS	−1.27	NS	NS	−1.32	NS	NS
MMP2					1.03	NS	NS	−1.33	NS	NS	−1.37	NS	NS
TIMP1					−1.19	NS	NS	1.37	NS	NS	1.06	NS	NS
CTNNB1					1.03	NS	NS	1.13	NS	NS	1.15	NS	NS
CD44					1.22	NS	NS	−1.06	NS	NS	−1.52	NS	NS
COL15A1					−1.11	NS	NS	1.26	NS	NS	−1.02	NS	NS
VCAN					1.31	NS	NS	−1.89	NS	NS	−1.32	NS	NS
CTGF					1.02	NS	NS	1.96	NS	NS	1.52	NS	NS
ITGAV					−1.02	NS	NS	−1.59	NS	NS	−1.39	NS	NS
COL6A2					−1.16	NS	NS	1.04	NS	NS	−1.19	NS	NS
CTNND1					−1.28	NS	NS	1.04	NS	NS	−1.15	NS	NS
LAMB1					1.20	NS	NS	1.08	NS	NS	1.12	NS	NS
ITGB1					−5.88	0.001	0.040	−2.56	NS	NS	−5.00	0.002	0.093
TIMP3					−1.05	NS	NS	1.16	NS	NS	1.20	NS	NS
THBS2					1.02	NS	NS	−1.16	NS	NS	1.14	NS	NS
ACTB					1.02	NS	NS	1.11	NS	NS	−1.82	NS	NS
COL16A1					1.15	NS	NS	1.64	NS	NS	1.44	NS	NS
NCAM1					1.11	NS	NS	1.02	NS	NS	−1.61	NS	NS
LAMC1					1.22	NS	NS	−1.08	NS	NS	−1.02	NS	NS
ITGB5					−1.27	NS	NS	1.18	NS	NS	−1.09	NS	NS
PECAM1					−1.72	NS	NS	−1.16	NS	NS	−1.04	NS	NS
ITGB4					−100.00	<0.001	0.004	−5.26	NS	NS	−50.00	<0.001	0.013
SPG7					1.17	NS	NS	−1.16	NS	NS	−1.04	NS	NS
SGCE					−1.06	NS	NS	1.30	NS	NS	−1.04	NS	NS
CTNNA1					1.22	NS	NS	1.21	NS	NS	1.24	NS	NS
ITGA1					−1.04	NS	NS	−1.08	NS	NS	−1.41	NS	NS
ITGA8					1.80	NS	NS	1.35	NS	NS	1.09	NS	NS
ITGB2					−1.96	0.039	NS	−1.79	NS	NS	−1.47	NS	NS
PGK1					−1.01	NS	NS	1.00	NS	NS	1.25	NS	NS
MMP14					1.05	NS	NS	−1.96	NS	NS	−1.69	NS	NS
LAMA3					1.05	NS	NS	1.10	NS	NS	−1.01	NS	NS
ITGA6					1.14	NS	NS	−1.16	NS	NS	1.61	NS	NS
SPP1					−2.17	NS	NS	−5.00	0.031	NS	−3.70	NS	NS
MMP11					1.42	NS	NS	−5.88	0.035	NS	−1.54	NS	NS
TBP					1.15	NS	NS	−1.12	NS	NS	−1.15	NS	NS
ITGA7					−1.20	NS	NS	1.00	NS	NS	−1.92	NS	NS
GUSB					1.00	NS	NS	−1.12	NS	NS	1.56	NS	NS
ITGB3					1.65	NS	NS	1.55	NS	NS	1.54	NS	NS
ITGA3					−1.92	NS	NS	−1.61	NS	NS	−1.54	NS	NS
ADAMTS1					1.52	NS	NS	2.45	NS	NS	2.72	NS	NS
ECM1					1.56	NS	NS	−1.09	NS	NS	2.69	0.044	NS
ITGA4					−1.43	NS	NS	−1.49	NS	NS	−1.25	NS	NS
MMP16					1.52	NS	NS	1.07	NS	NS	1.25	NS	NS
SELP					1.20	NS	NS	1.73	NS	NS	1.95	NS	NS
HPRT1					1.06	NS	NS	1.07	NS	NS	1.06	NS	NS
ITGAM					−1.12	NS	NS	1.08	NS	NS	1.19	NS	NS
CLEC3B					1.03	NS	NS	1.64	NS	NS	2.06	NS	NS
VCAM1					1.34	NS	NS	1.94	NS	NS	1.50	NS	NS
MMP9					−1.04	NS	NS	−10.00	0.024	NS	−1.33	NS	NS
HMBS					−1.09	NS	NS	1.53	NS	NS	−1.22	NS	NS
LAMA2					−1.41	NS	NS	1.62	NS	NS	1.40	NS	NS
COL14A1					−1.06	NS	NS	1.83	NS	NS	1.25	NS	NS
KAL1					1.15	NS	NS	−1.04	NS	NS	−1.04	NS	NS
CNTN1					1.68	NS	NS	2.63	0.036	NS	2.58	0.040	NS
ITGAL					−1.64	NS	NS	−1.16	NS	NS	1.08	NS	NS
ADAMTS13					1.61	NS	NS	1.16	NS	NS	1.56	NS	NS
MMP15					1.09	NS	NS	1.21	NS	NS	1.61	NS	NS
COL6A1					2.34	0.038	NS	2.05	NS	NS	1.46	NS	NS
COL11A1					−1.54	NS	NS	−1.19	NS	NS	−1.96	0.045	NS
COL5A1					2.04	NS	NS	1.73	NS	NS	2.21	NS	NS
ICAM1					1.31	NS	NS	−1.35	NS	NS	1.38	NS	NS
COL8A1					1.54	NS	NS	1.13	NS	NS	1.54	NS	NS
MMP13					−2.38	NS	NS	−33.33	0.013	NS	−25.00	0.020	NS
VTN					1.05	NS	NS	1.14	NS	NS	−1.18	NS	NS
COL7A1					−1.01	NS	NS	−1.28	NS	NS	1.87	NS	NS
LAMA1					−1.85	NS	NS	−1.30	NS	NS	−1.19	NS	NS
ITGA2					2.40	NS	NS	1.64	NS	NS	2.31	NS	NS
ADAMTS8					1.19	NS	NS	−1.03	NS	NS	1.90	NS	NS
CDH1					−1.45	NS	NS	−11.11	0.020	NS	−1.20	NS	NS
THBS3					−1.33	NS	NS	1.71	NS	NS	1.00	NS	NS
MMP7					−1.67	NS	NS	1.33	NS	NS	2.04	NS	NS
SELE					1.05	NS	NS	2.74	NS	NS	1.87	NS	NS
MMP10					−3.23	NS	NS	−50.00	0.017	NS	−1.47	NS	NS
SELL					1.31	NS	NS	1.43	NS	NS	1.93	NS	NS
LAMB3					−1.01	NS	NS	−2.13	0.046	NS	1.72	NS	NS
MMP3					5.23	NS	NS	−1.28	NS	NS	2.47	NS	NS
CTNND2					1.08	NS	NS	1.49	NS	NS	7.60	0.042	NS
HAS1	ND	ND	ND	ND	NA	NA	NA	NA	NA	NA	NA	NA	NA
MMP1	ND	ND	ND	ND	NA	NA	NA	NA	NA	NA	NA	NA	NA
MMP12	ND	ND	ND	ND	NA	NA	NA	NA	NA	NA	NA	NA	NA
MMP8	ND	ND	ND	ND	NA	NA	NA	NA	NA	NA	NA	NA	NA

Figure 1 – Human extracellular matrix and adhesion molecule quantitative polymerase chain reaction arrays on five samples per group: heatmap and statistical analysis. Heatmap of 84 tested extracellular matrix-related genes sorted on the basis of their relative abundance in the untreated group (green for more expressed, red for less expressed). Fold change (FC), *P*-values and *Q*-values are presented, and significant differences ($P < 0.05$, $Q < 0.10$) are highlighted. CTL, untreated; LT, long-term UPA-responsive; NR, UPA-nonresponsive; ST, short-term UPA-responsive.

other MMPs (*MMP9*, *MMP10*, *MMP11* and *MMP13*) showed lower expression levels after UPA treatment, mainly in the long-term group compared with controls (*MMP9*: FC = –10.00, $P = 0.024$; *MMP10*: FC = –50.00, $P = 0.017$; *MMP11*: FC = –5.88, $P = 0.035$; *MMP13*: FC = –33.33, $P = 0.013$. No difference remained significant after statistical adjustment, $Q > 0.100$). Expression levels of ADAMTS family members (other metzincin proteases) were found to be stable in all four groups.

Adhesion molecules (including *ITGA5*, *THBS1*, *CTNNB1*, *CD44*) figured among the third group of the most highly transcribed genes. Two members of the β-integrin subfamily (*ITGB4* and *ITGB1*) showed strong and significant downregulation in UPA-treated tissues and, more specially, in the short-term group compared with controls (*ITGB1*: FC = –5.88, $P = 0.001$, $Q = 0.040$; *ITGB4*: FC = –100.00, $P < 0.001$, $Q = 0.004$) (**Figure 1**). Another adhesion molecule, E-cadherin (*CDH1*), had a tendency towards repression in the long-term group, but not in short-term or non-responsive groups compared with controls.

Apoptosis-related genes differentially expressed after ulipristal acetate treatment

Differential gene expression for 94 genes involved in cell death was evaluated in all four groups using the human apoptosis arrays. On the whole, most candidate genes were found to be moderately transcribed compared with structural ECM genes, or even undetected. Myomas from all groups expressed both anti- and proapoptotic factors (for the most strongly expressed antiapoptotic genes *NAIP*, *BIRC8*, *PEA15*, *BCL2*; for the most strongly expressed proapoptotic genes *BNIP3L*, *BCL2L11*, *BAX*), without any difference between groups ($Q > 0.100$) (**Figure 2**).

Only 10 genes (*BOK*, *BIRC2*, *BIRC5*, *BIRC8*, *CASP8*, *IKBKE*, *LTA*, *NFKBIE*, *RIPK1* and *XIAP*) showed a statistically significant *P*-value (between $P = 0.043$ and $P = 0.008$) in at least one of the UPA-treated groups versus controls, but none remained significant after adjustment for multiple testing ($Q > 0.100$) (**Figure 2**). Among these genes, *BIRC5*, *BIRC8*, *BOK* and *XIAP* had the strongest modulations (FC >3.5).

Apoptosis inhibitor *BIRC5* demonstrated the strongest modulation among these genes, with a significant downregulation in UPA-ST responsive group compared with controls (FC = –4.35, $P = 0.038$, $Q > 0.100$) (**Figure 2**).

Quantitative PCR extension on additional samples

Taking into account PCR array results, 11 genes were selected on the basis of either their statistical *P*-values, differential expression between responsive and non-responsive myomas, or unexpected modulations. These genes were then analysed by real-time qPCR on nine samples per group to validate the PCR array results (Supplementary Figure S1). This analysis confirmed significant differences between the groups in expression of four genes (*TNC*, *ITGB4*,

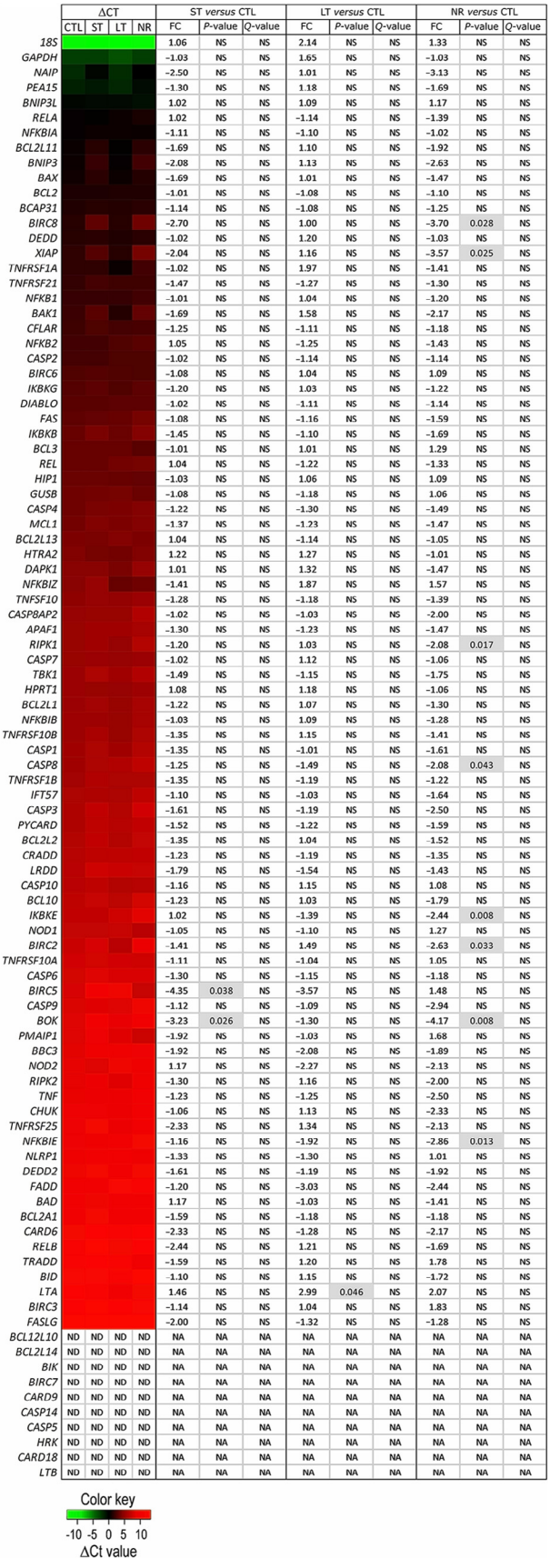

	ΔCT				ST *versus* CTL			LT *versus* CTL			NR *versus* CTL		
	CTL	ST	LT	NR	FC	*P*-value	Q-value	FC	*P*-value	Q-value	FC	*P*-value	Q-value
18S					1.06	NS	NS	2.14	NS	NS	1.33	NS	NS
GAPDH					−1.03	NS	NS	1.65	NS	NS	−1.03	NS	NS
NAIP					−2.50	NS	NS	1.01	NS	NS	−3.13	NS	NS
PEA15					−1.30	NS	NS	1.18	NS	NS	−1.69	NS	NS
BNIP3L					1.02	NS	NS	1.09	NS	NS	1.17	NS	NS
RELA					1.02	NS	NS	−1.14	NS	NS	−1.39	NS	NS
NFKBIA					−1.11	NS	NS	−1.10	NS	NS	−1.02	NS	NS
BCL2L11					−1.69	NS	NS	1.10	NS	NS	−1.92	NS	NS
BNIP3					−2.08	NS	NS	1.13	NS	NS	−2.63	NS	NS
BAX					−1.69	NS	NS	1.01	NS	NS	−1.47	NS	NS
BCL2					−1.01	NS	NS	−1.08	NS	NS	−1.10	NS	NS
BCAP31					−1.14	NS	NS	−1.08	NS	NS	−1.25	NS	NS
BIRC8					−2.70	NS	NS	1.00	NS	NS	−3.70	0.028	NS
DEDD					−1.02	NS	NS	1.20	NS	NS	−1.03	NS	NS
XIAP					−2.04	NS	NS	1.16	NS	NS	−3.57	0.025	NS
TNFRSF1A					−1.02	NS	NS	1.97	NS	NS	−1.41	NS	NS
TNFRSF21					−1.47	NS	NS	−1.27	NS	NS	−1.30	NS	NS
NFKB1					−1.01	NS	NS	1.04	NS	NS	−1.20	NS	NS
BAK1					−1.69	NS	NS	1.58	NS	NS	−2.17	NS	NS
CFLAR					−1.25	NS	NS	−1.11	NS	NS	−1.18	NS	NS
NFKB2					1.05	NS	NS	−1.25	NS	NS	−1.43	NS	NS
CASP2					−1.02	NS	NS	−1.14	NS	NS	−1.14	NS	NS
BIRC6					−1.08	NS	NS	1.04	NS	NS	1.09	NS	NS
IKBKG					−1.20	NS	NS	1.03	NS	NS	−1.22	NS	NS
DIABLO					−1.02	NS	NS	−1.11	NS	NS	−1.14	NS	NS
FAS					−1.08	NS	NS	−1.16	NS	NS	−1.59	NS	NS
IKBKB					−1.45	NS	NS	−1.10	NS	NS	−1.69	NS	NS
BCL3					−1.01	NS	NS	1.01	NS	NS	1.29	NS	NS
REL					1.04	NS	NS	−1.22	NS	NS	−1.33	NS	NS
HIP1					−1.03	NS	NS	1.06	NS	NS	1.09	NS	NS
GUSB					−1.08	NS	NS	−1.18	NS	NS	1.06	NS	NS
CASP4					−1.22	NS	NS	−1.30	NS	NS	−1.49	NS	NS
MCL1					−1.37	NS	NS	−1.23	NS	NS	−1.47	NS	NS
BCL2L13					1.04	NS	NS	−1.14	NS	NS	−1.05	NS	NS
HTRA2					1.22	NS	NS	1.27	NS	NS	−1.01	NS	NS
DAPK1					1.01	NS	NS	1.32	NS	NS	−1.47	NS	NS
NFKBIZ					−1.41	NS	NS	1.87	NS	NS	1.57	NS	NS
TNFSF10					−1.28	NS	NS	−1.18	NS	NS	−1.39	NS	NS
CASP8AP2					−1.02	NS	NS	−1.03	NS	NS	−2.00	NS	NS
APAF1					−1.30	NS	NS	−1.23	NS	NS	−1.47	NS	NS
RIPK1					−1.20	NS	NS	1.03	NS	NS	−2.08	0.017	NS
CASP7					−1.02	NS	NS	1.12	NS	NS	−1.06	NS	NS
TBK1					−1.49	NS	NS	−1.15	NS	NS	−1.75	NS	NS
HPRT1					1.08	NS	NS	1.18	NS	NS	−1.06	NS	NS
BCL2L1					−1.22	NS	NS	1.07	NS	NS	−1.30	NS	NS
NFKBIB					−1.03	NS	NS	1.09	NS	NS	−1.28	NS	NS
TNFRSF10B					−1.35	NS	NS	1.15	NS	NS	−1.41	NS	NS
CASP1					−1.35	NS	NS	−1.01	NS	NS	−1.61	NS	NS
CASP8					−1.25	NS	NS	−1.49	NS	NS	−2.08	0.043	NS
TNFRSF1B					−1.35	NS	NS	−1.19	NS	NS	−1.22	NS	NS
IFT57					−1.10	NS	NS	−1.03	NS	NS	−1.64	NS	NS
CASP3					−1.61	NS	NS	−1.19	NS	NS	−2.50	NS	NS
PYCARD					−1.52	NS	NS	−1.22	NS	NS	−1.59	NS	NS
BCL2L2					−1.35	NS	NS	1.04	NS	NS	−1.52	NS	NS
CRADD					−1.23	NS	NS	−1.19	NS	NS	−1.35	NS	NS
LRDD					−1.79	NS	NS	−1.54	NS	NS	−1.43	NS	NS
CASP10					−1.16	NS	NS	1.15	NS	NS	1.08	NS	NS
BCL10					−1.23	NS	NS	1.03	NS	NS	−1.79	NS	NS
IKBKE					1.02	NS	NS	−1.39	NS	NS	−2.44	0.008	NS
NOD1					−1.05	NS	NS	−1.10	NS	NS	1.27	NS	NS
BIRC2					−1.41	NS	NS	1.49	NS	NS	−2.63	0.033	NS
TNFRSF10A					−1.11	NS	NS	−1.04	NS	NS	1.05	NS	NS
CASP6					−1.30	NS	NS	−1.15	NS	NS	−1.18	NS	NS
BIRC5					−4.35	0.038	NS	−3.57	NS	NS	1.48	NS	NS
CASP9					−1.12	NS	NS	−1.09	NS	NS	−2.94	NS	NS
BOK					−3.23	0.026	NS	−1.30	NS	NS	−4.17	0.008	NS
PMAIP1					−1.92	NS	NS	−1.03	NS	NS	1.68	NS	NS
BBC3					−1.92	NS	NS	−2.08	NS	NS	−1.89	NS	NS
NOD2					1.17	NS	NS	−2.27	NS	NS	−2.13	NS	NS
RIPK2					−1.30	NS	NS	1.16	NS	NS	−2.00	NS	NS
TNF					−1.23	NS	NS	−1.25	NS	NS	−2.50	NS	NS
CHUK					−1.06	NS	NS	1.13	NS	NS	−2.33	NS	NS
TNFRSF25					−2.33	NS	NS	1.34	NS	NS	−2.13	NS	NS
NFKBIE					−1.16	NS	NS	−1.92	NS	NS	−2.86	0.013	NS
NLRP1					−1.33	NS	NS	−1.30	NS	NS	1.01	NS	NS
DEDD2					−1.61	NS	NS	−1.19	NS	NS	−1.92	NS	NS
FADD					−1.20	NS	NS	−3.03	NS	NS	−2.44	NS	NS
BAD					1.17	NS	NS	−1.03	NS	NS	−1.41	NS	NS
BCL2A1					−1.59	NS	NS	−1.18	NS	NS	−1.18	NS	NS
CARD6					−2.33	NS	NS	−1.28	NS	NS	−2.17	NS	NS
RELB					−2.44	NS	NS	1.21	NS	NS	−1.69	NS	NS
TRADD					−1.59	NS	NS	1.20	NS	NS	1.78	NS	NS
BID					−1.10	NS	NS	1.15	NS	NS	−1.72	NS	NS
LTA					1.46	NS	NS	2.99	0.046	NS	2.07	NS	NS
BIRC3					−1.14	NS	NS	1.04	NS	NS	1.83	NS	NS
FASLG					−2.00	NS	NS	−1.32	NS	NS	−1.28	NS	NS
BCL12L10	ND	ND	ND	ND	NA	NA	NA	NA	NA	NA	NA	NA	NA
BCL2L14	ND	ND	ND	ND	NA	NA	NA	NA	NA	NA	NA	NA	NA
BIK	ND	ND	ND	ND	NA	NA	NA	NA	NA	NA	NA	NA	NA
BIRC7	ND	ND	ND	ND	NA	NA	NA	NA	NA	NA	NA	NA	NA
CARD9	ND	ND	ND	ND	NA	NA	NA	NA	NA	NA	NA	NA	NA
CASP14	ND	ND	ND	ND	NA	NA	NA	NA	NA	NA	NA	NA	NA
CASP5	ND	ND	ND	ND	NA	NA	NA	NA	NA	NA	NA	NA	NA
HRK	ND	ND	ND	ND	NA	NA	NA	NA	NA	NA	NA	NA	NA
CARD18	ND	ND	ND	ND	NA	NA	NA	NA	NA	NA	NA	NA	NA
LTB	ND	ND	ND	ND	NA	NA	NA	NA	NA	NA	NA	NA	NA

Figure 2 – Human apoptosis quantitative polymerase chain reaction arrays on five samples per group: heatmap and statistical analysis. Heatmap of 92 tested apoptosis-related genes sorted based on their relative abundance in the untreated group (green for strongly expressed, red for faintly expressed). Fold change (FC), *P*-values and *Q*-values are presented, and significant differences ($P < 0.05$, $Q < 0.10$) are highlighted. CTL, untreated; LT, long-term UPA-responsive; NR, UPA-non-responsive; ST, short-term UPA-responsive).

BIRC5 and *CTNND2*) (**Table 1**). *ITGB4* was much less extensively expressed (up to 20-fold for short-term group, $P < 0.001$, $Q < 0.001$) in UPA-treated samples compared with untreated controls (UPA-treated versus CTL: FC = −12.50, $P < 0.001$, $Q < 0.001$). Considering the response to UPA, the *BIRC5* gene was markedly down-expressed in myomas responsive to short-term treatment compared with CTL samples (ST: FC = −7.69, $P < 0.001$, $Q = 0.010$), but this was not the case in the long-term and non-responsive groups. When both responsive groups (short-term and long-term) were combined, the *TNC* gene was significantly repressed compared with controls (FC = −2.50, $P = 0.010$; $Q = 0.090$) (**Table 1**). On the contrary, only non-responsive samples were confirmed to express roughly seven times more of the *CTNND2* gene than untreated myomas (NR: FC = +7.36, $P < 0.001$, $Q = 0.010$) or UPA-responsive myomas (non-responsive versus responsive groups as a whole: FC = +5.26, $P < 0.001$, $Q = 0.010$).

Discussion

Significant (≥25%) and sustained regression of most myomas is typically observed in 80% of patients after UPA treatment (Donnez and Dolmans, 2016). We previously reported that UPA treatment was able to induce multifactorial events, including a slight decrease in proliferation, temporary induction of apoptosis and reduction of the ECM presumed to be caused by MMP activity (Courtoy et al., 2015). These modifications could play a role in the long-lasting benefits of UPA in terms of myoma shrinkage (Donnez *et al.*, 2012b). The present work aimed to characterize the molecular response of myomas by comparing expression of cell death or ECM-related genes in myomas undergoing significant shrinkage under UPA versus non-responsive and untreated myomas.

PCR arrays for multiple candidate gene screening

First, identification of *HPRT1* as the best reference gene is wholly in line with similar studies that found comparable expression levels of this gene between the myometrium and myoma cells (Almeida et al., 2014), hence confirming its role as a reference gene for myomas.

Having met this prerequisite, 176 candidate genes were selected owing to their known role in apoptotic signalling pathways or ECM remodelling, or even on the basis of in-vitro studies, and compared. By and large, only two genes (*ITGB1* and *ITGB4*) showed expression change after UPA treatment, but their expression was similar between responsive and non-responsive groups. A number of other genes, however, had interesting profiles with differential expression in responsive or non-responsive groups. For this reason, all gene expression results were scrutinized according to three criteria: (1) their *Q*-values; (2) observed opposing tendencies between

Table 1 – Validation of 11 gene expression results from nine samples per group and multiple comparisons. Genes were sorted on the basis of their abundance in the untreated group. Gene expression was normalized to the hypoxanthine phosphoribosyltransferase 1 (*HPRT1*) gene.

Gene name	Treatment			Response									Sustained effect		
	Treated *versus* CTL			ST *versus* CTL			LT *versus* CTL			(ST + LT) *versus* CTL			LT *versus* ST		
	FC	P-value	Q-value	FC	P-value	Q-value	FC	P-value	Q-value	FC	P-value	Q-value	FC	P-value	Q-value
TNC	−2.04	NS	NS	−2.32	0.040	NS	−2.70	0.020	NS	−2.50	0.010	0.090	−1.16	NS	NS
ITGB1	−2.17	NS	NS	−3.03	NS	NS	−2.08	NS	NS	−2.50	NS	NS	1.47	NS	NS
ITGB4	−12.50	<0.001	<0.001	−20.00	<0.001	<0.001	−7.14	0.000	0.040	−11.11	<0.001	<0.001	2.70	NS	NS
LAMB3	1.02	NS	NS	−1.03	NS	NS	−1.14	NS	NS	−1.08	NS	NS	−1.11	NS	NS
CTNND2	2.47	NS	NS	1.62	NS	NS	1.27	NS	NS	1.43	NS	NS	−1.28	NS	NS
MMP9	−1.36	NS	NS	1.01	NS	NS	−3.44	NS	NS	−1.85	NS	NS	−3.57	NS	NS
MMP10	−1.63	NS	NS	−2.77	NS	NS	−3.70	NS	NS	−3.22	NS	NS	−1.35	NS	NS
MMP13	1.24	NS	NS	1.95	NS	NS	−1.81	NS	NS	1.03	NS	NS	−3.57	NS	NS
BIRC5	−2.32	NS	NS	−7.69	<0.001	0.010	−1.44	NS	NS	−3.33	0.020	NS	5.51	<0.001	0.020
BIRC3	1.15	NS	NS	−1.25	NS	NS	−1.21	NS	NS	−1.23	NS	NS	1.02	NS	NS
CASP3	−1.11	NS	NS	−1.23	NS	NS	1.32	NS	NS	1.03	NS	NS	1.64	NS	NS

Gene name	No response											
	NR *versus* CTL			(ST + LT) *versus* NR			ST *versus* NR			LT *versus* NR		
	FC	P-value	Q-value	FC	P-value	Q-value	FC	P-value	Q-value	FC	P-value	Q-value
TNC	−1.31	NS	NS	−1.92	NS	NS	−1.78	NS	NS	−2.04	NS	NS
ITGB1	−1.61	NS	NS	−1.5625	NS	NS	−1.88	NS	NS	−1.28	NS	NS
ITGB4	−12.50	<0.001	0.010	1.11	NS	NS	−1.47	NS	NS	1.82	NS	NS
LAMB3	1.25	NS	NS	−1.36	NS	NS	−1.29	NS	NS	−1.42	NS	NS
CTNND2	7.36	<0.001	0.010	−5.26	<0.001	0.010	−4.54	0.010	0.040	−5.88	<0.001	0.020
MMP9	1.36	NS	NS	−2.50	NS	NS	−1.33	NS	NS	−4.76	0.050	NS
MMP10	2.45	NS	NS	−7.69	0.030	NS	−6.66	NS	NS	−9.09	0.040	NS
MMP13	1.81	NS	NS	−1.75	NS	NS	1.08	NS	NS	−3.33	NS	NS
BIRC5	−1.13	NS	NS	−2.94	0.040	NS	−7.14	<0.001	0.010	−1.26	NS	NS
BIRC3	2.34	NS	NS	−2.85	0.020	NS	−2.94	0.040	NS	−2.85	0.040	NS
CASP3	−1.47	NS	NS	1.52	NS	NS	1.19	NS	NS	1.95	NS	NS

CTL, untreated; FC, fold change; LT, long-term UPA-responsive; NR, UPA-non-responsive; ST, short-term UPA-responsive.

responsive and non-responsive groups; and (3) important biological functions already reported. This selection rationale identified 11 genes, which were further tested by quantitative reverse transcription PCR on additional myoma samples to increase the power of the analysis and better mimic naturally occurring heterogeneity.

Progesterone-sensitive genes modulated by ulipristal acetate

Both β1 and β4 integrins demonstrated patterns of repression after UPA treatment, especially regarding *ITGB4*. These genes are progesterone-controlled (Cao et al., 2007), strongly suggesting that UPA interferes with this regulation. As recently reported by Malik et al. (2012), myoma cells overexpress integrins β1 and α6, and these subunits dimerize to form a specific laminin receptor and allow mechanotransduction signals. Integrin–laminin interaction was indeed shown to be essential for myoma cell proliferation and subsequent tissue organization (Chen et al., 2013; Malik et al., 2012). Although integrin β4 function has not yet been investigated in the context of uterine myomas, it is known to have tumourigenic properties when combined with laminin5-β3 (Dajee et al., 2003). The present results, therefore, suggest that UPA potentially counteracts proliferation and survival by disrupting aberrant integrin signalling, calling for functional studies to be conducted.

Differential gene expression according to ulipristal acetate -response

Responsive myomas express less TNC

Only responsive myomas showed significant repression of the *TNC* gene. Similarly to *ITGB1* and *ITGB4*, this gene is directly regulated by progesterone (Tamm et al., 2009) and overexpressed in myomas (Bogusiewicz et al., 2012). TNC association with the integrin β1 subunit promotes cell proliferation, tumourigenesis and fibrosis (Tucker and Chiquet-Ehrismann, 2015). These elements suggest that tenascin-C plays a role with integrins in the pathogenesis of myomas and that *TNC* repression may contribute to tumour regression after UPA treatment.

Short-term responsive myomas express less BIRC5

In the present study, we report differential gene regulation of survivin (*BIRC5*), with significant repression observed in short-term UPA-responsive tumours compared with controls or with non-responsive myomas (**Table 1**). *BIRC5* and *BIRC3* belong to the inhibitor of apoptosis (IAP) gene family and interact with caspase-3, -7 and -8 to inhibit their apoptotic activity. Consequently, loss of IAPs releases a brake in these apoptotic cascades and facilitates cell death, which may explain the higher apoptotic levels seen in UPA-responsive myomas, as suggested elsewhere for another SPRM (Sasaki et al., 2007). Repression of *BIRC5* in the short-term group only is also consistent with the fact that apoptosis mainly occurs during the first course of treatment (Courtoy et al., 2015), suggesting a 'selective-step' by the most UPA-sensitive cells with lower levels of IAP. On the contrary, non-responsive myomas could mediate their resistance to UPA-induced cell death by maintaining IAP levels.

CTNND2 *is more extensively expressed in non-responsive myomas*

Catenin delta subunit 2 (*CTNND2*) was significantly upregulated in the non-responsive group, but this was not the case in UPA-responsive myomas. Biologically, besides its widely known role in cell adhesion, δ-catenin resembles β-catenin in directly controlling expression of proliferation-associated genes, namely inducing the cell cycle facilitator *cyclin D1* and pro-survival *BIRC5* genes (Kim et al., 2012; Zeng et al., 2009) by means of the Wnt signalling pathway (Nopparat et al., 2015). Interestingly, this pathway is essential for proliferation of myoma progenitor cells, which are deficient in progesterone receptors (Ono et al., 2013), and therefore not presumed to be UPA-sensitive. Hence, one hypothesis could be that these tumours expressing high CTNND2 levels would proliferate more extensively, possibly because of an initially larger pool of UPA-insensitive myoma progenitor cells (Drosch et al., 2014), explaining the lack of regression or continued growth under UPA therapy in non-responsive myomas.

Candidate genes not modulated by ulipristal acetate in vivo

BCL-2 *and* CASP3 *are not affected by ulipristal acetate* in vivo

In the present study, *BCL-2* mRNA expression in myomas was not modulated by UPA (**Figure 2**). This result corroborates our study and other recent in-vivo studies at the mRNA and protein level (Courtoy et al., 2017; Yun et al., 2015), but does not confirm results based on very short-time limited UPA-exposure in cell culture, which suggested *BCL-2* repression by UPA (Xu et al., 2005) or mifepristone (Yin et al., 2012) to be key factor in explaining apoptosis. In our study, UPA treatment did not stimulate caspase synthesis (especially *CASP3*) (**Figure 2**), indicating that preoperative UPA treatment does not induce caspase-dependent apoptosis, as previously reported (Courtoy et al., 2015). One possible explanation for these discrepancies between in-vitro- and in-vivo studies is that daily exposure to UPA in patients over several months would result in the selection of the most UPA-resistant cells. Hence, UPA-induced cell death might well be more complex than in-vitro studies infer, potentially occurring through other cell-death pathways (Courtoy et al., 2015).

Extracellular matrix structural gene expression are not changed by ulipristal acetate in vivo

Concerning ECM components, the relatively high expression levels of collagens (*COL4A2*, *COL1A1* and *COL12A1*) and fibronectin (*FN1*) found in untreated myomas (**Figure 1**) is consistent with the other published reports (Leppert et al., 2006). In contrast with two-dimensional in-vitro study findings, UPA therapy did not change their expression, which showed a reduction in collagen content in myoma cells treated with UPA (Xu et al., 2008). Consequently, shrinkage of myomas might be less imputable to repression of collagen and fibronectin synthesis, but more to their protein resorption, presumably by protease activity.

Expression levels of MMP genes are not consistently regulated by ulipristal acetate in vivo

We previously reported that UPA therapy led to increased levels of MMP-2 protein expression in myomas (Courtoy et al., 2015), and found higher levels of MMP activity in responsive tumours than non-responsive or untreated samples (Courtoy et al., 2018), supporting the notion of an MMP-based mechanism for ECM resorption. In the present study, however, expression of the *MMP2* gene was unchanged between groups and no significant difference was found for other relevant MMP. Nevertheless, discrepant regulation between mRNA and protein expression for MMP is common and might be attributed to post-translational regulation (Sternlicht and Werb, 2001).

Indeed, MMP function is dynamic and precisely controlled in-vivo by mRNA stability regulation and post-translational modifications conferring higher protein stability; formation of complexes with other MMP; the relative abundance of their inhibitors (TIMPs); or even by means of recapture and degradation by cells (Selvais et al., 2009). Therefore, higher levels of MMP proteins after UPA treatment are likely to be caused by non-transcriptomic regulations.

Strengths and limitations

To determine whether factors involved in apoptotic or ECM-related signalling pathways are regulated by UPA on a genomic level, a PCR array approach was chosen because of the advantage of investigating a panel of relevant genes involved in apoptosis and ECM-related signalling pathways, hence avoiding evaluation of irrelevant signalling pathways; the possibility of analysing other genes involved in these signalling pathways that have not been considered in the literature on in-vitro studies; and its high reproducibility and ability to use multiple HKG. Nevertheless, all transcriptomic analyses are inherently limited to showing gene expression, which does not identify non-genomic regulation or protein content. Of course, our targeted strategy does not provide complete transcriptomic screening and likely misses other gene expression regulated by UPA.

The second limitation resides in comparing different myomas from different patients, inevitably introducing a degree of variability to the study. Our study samples may have different genetic backgrounds, as *MED12* is mutated in up to 70% of common myomas (Mehine et al., 2013; Sandberg, 2005). Indeed, *MED12* mutation is speculated to be a primary genomic alteration causing genomic instability and promoting myoma development (Mittal et al., 2015; Yatsenko et al., 2017). Although the likelihood that *MED12* mutation in turn influences the response of uterine myomas to UPA is low, it cannot be ruled out. This should be addressed in future studies, as should the effect of more complex chromosomal rearrangements affecting specific loci, such as *HMGA2* (chromosome 12) or *COL4A5* and *COL4A6* (chromosome X) (Mehine et al., 2013; Sandberg, 2005).

Another limitation of our study is possibly the small number of samples available for comparison. In order to meet all inclusion criteria, particularly the rigorously defined evaluation of response obtained after multiple magnetic resonance imaging, the number of eligible participants was limited and patients showed variable timing between the end of treatment and surgery. On the one hand, because UPA clearance is relatively fast, it is conceivable that transitory regulation of gene expression directly depending on circulating levels of UPA could not be detected. On the other hand, gene expression regulation was hypothesized to be stable after treatment, as UPA-responsive myomas maintain long-lasting reductions in volume. Moreover, such enduring effects are likely to be mediated by epigenetic modifications. Further studies with larger numbers of well-characterized samples are clearly needed to evaluate the biological role of UPA in other patient populations.

In conclusion, UPA treatment significantly modifies expression of four genes in myomas: *ITGB4* expression is repressed by UPA; *TNC* expression is downregulated in UPA-responsive tumours; *BIRC5* is repressed in UPA-responsive myomas, but only during the first months of treatment when apoptosis occurs; and myomas non-responsive to UPA upregulate *CTNND2* gene expression. This characterization provides the first molecular distinction between myomas responsive or non-responsive to UPA treatment, deepening our knowledge of UPA mechanisms of action in uterine myomas and enhancing our understanding of the disease itself.

Acknowledgement

The authors thank Jean Squifflet, Pascal Jadoul and Amandine Gerday from the Gynaecology Department of Cliniques Universitaires Saint-Luc for their help with sample collection; Bertrand Bearzatto and all members of the Centre de Technologies Moléculaires Appliquées for their support with biomolecular analyses; Dolores Gonzalez, Olivier Van Kerk, for their technical assistance; Patrick Henriet, Christophe Pierreux and Diego Manavella for their scientific contribution and constructive criticism; Deborah Godefroidt for administrative help; and Mira Hryniuk for reviewing the English language of the manuscript. This work was supported by funds from the F.R.S-FNRS/FRIA awarded to GEC [grant number FC005053] and the F.R.S.M-FNRS to MMD [grant number 5/4/150/5]. Transcriptomic analysis was supported by PregLem (Geneva, Switzerland). Funds for research were provided by PregLem through an unrestricted grant. The fund providers played no role in the collection, analysis or interpretation of data, nor in the writing of the report.

Appendix: Supplementary material

Supplementary data to this article can be found online at doi:10.1016/j.rbmo.2018.04.050.

ARTICLE INFO

Article history:
Received 2 October 2017
Received in revised form 19 April 2018
Accepted 20 April 2018
Declaration: GEC received a scholarship from PregLem (Geneva, Switzerland) between 2013 and 2015. JD has been a member of the Scientific Advisory Board of PregLem since 2007. PA is Vice President Medical Affairs at Gedeon Richter-PregLem. JA, EM, ML, and MMD have nothing to disclose.

Keywords:
Apoptosis
Clinical response
Extracellular matrix
qPCR arrays
Ulipristal acetate
Uterine myomas

REFERENCES

Almeida, T.A., Quispe-Ricalde, A., Montes de Oca, F., Foronda, P., Hernandez, M.M., 2014. A high-throughput open-array qPCR gene panel to identify housekeeping genes suitable for myometrium and leiomyoma expression analysis. Gynecol. Oncol. 134, 138–143.

Bogusiewicz, M., Semczuk, A., Juszczak, M., Langner, E., Walczak, K., Rzeski, W., Tomaszewski, J., Rechberger, T., 2012. Expression of matricellular proteins in human uterine leiomyomas and normal myometrium. Histol. Histopathol. 27, 1495–1502.

Cao, W., Mah, K., Carroll, R.S., Slayden, O.D., Brenner, R.M., 2007. Progesterone withdrawal up-regulates fibronectin and integrins during menstruation and repair in the rhesus macaque endometrium. Hum. Reprod. 22, 3223–3231.

Chen, H.M., Lin, Y.H., Cheng, Y.M., Wing, L.Y., Tsai, S.J., 2013. Overexpression of integrin-beta1 in leiomyoma promotes cell spreading and proliferation. J. Clin. Endocrinol. Metab. 98, E837–E846.

Commandeur, A.E., Styer, A.K., Teixeira, J.M., 2015. Epidemiological and genetic clues for molecular mechanisms involved in uterine leiomyoma development and growth. Hum. Reprod. Update 21, 593–615.

Courtoy, G.E., Donnez, J., Marbaix, E., Dolmans, M.M., 2015. In vivo mechanisms of uterine myoma volume reduction with ulipristal acetate treatment. Fertil. Steril. 104, 426–434, e421.

Courtoy, G.E., Donnez, J., Marbaix, E., Barreira, M., Luyckx, M., Dolmans, M.M., 2017. Progesterone receptor isoforms, nuclear cofactors NCoR1 and SRC1, and Bcl-2 and Akt/p-Akt in uterine myomas after ulipristal acetate treatment: a systematic immunohistochemical evaluation. Gynecol. Obstet. Invest. [Epub ahead of print].

Courtoy, G.E., Henriet, P., Marbaix, E., de Codt, M., Luyckx, M., Donnez, J., Dolmans, M.M., 2018. Matrix metalloproteinase activity correlates with uterine myoma volume reduction after ulipristal acetate treatment. J. Clin. Endocrinol. Metab. 103, 1566–1573.

Dajee, M., Lazarov, M., Zhang, J.Y., Cai, T., Green, C.L., Russell, A.J., Marinkovich, M.P., Tao, S., Lin, Q., Kubo, Y., Khavari, P.A., 2003. NF-kappaB blockade and oncogenic Ras trigger invasive human epidermal neoplasia. Nature 421, 639–643.

Dallas, P.B., Gottardo, N.G., Firth, M.J., Beesley, A.H., Hoffmann, K., Terry, P.A., Freitas, J.R., Boag, J.M., Cummings, A.J., Kees, U.R., 2005. Gene expression levels assessed by oligonucleotide microarray analysis and quantitative real-time RT-PCR – how well do they correlate? BMC Genomics 6, 59.

Donnez, J., Dolmans, M.M., 2016. Uterine fibroid management: from the present to the future. Hum. Reprod. Update 22, 665–686.

Donnez, J., Tatarchuk, T.F., Bouchard, P., Puscasiu, L., Zakharenko, N.F., Ivanova, T., Ugocsai, G., Mara, M., Jilla, M.P., Bestel, E., Osterloh, I., Loumaye, E., PEARL I Study Group, 2012a. Ulipristal acetate versus placebo for fibroid treatment before surgery. N. Engl. J. Med. 366, 409–420.

Donnez, J., Tomaszewski, J., Vazquez, F., Bouchard, P., Lemieszczuk, B., Baro, F., Nouri, K., Selvaggi, L., Sodowski, K., Bestel, E., Terrill, P., Osterloh, I., Loumaye, E., PEARL II Study Group, 2012b. Ulipristal acetate versus leuprolide acetate for uterine fibroids. N. Engl. J. Med. 366, 421–432.

Donnez, J., Vazquez, F., Tomaszewski, J., Nouri, K., Bouchard, P., Fauser, B.C., Barlow, D.H., Palacios, S., Donnez, O., Bestel, E., Osterloh, I., Loumaye, E., PEARL III and PEARL III Extension Study Group, 2014. Long-term treatment of uterine fibroids with ulipristal acetate. Fertil. Steril. 101, 1565–1573, e1561-1518.

Donnez, J., Arriagada, P., Donnez, O., Dolmans, M.M., 2015. Current management of myomas: the place of medical therapy with the advent of selective progesterone receptor modulators. Curr. Opin. Obstet. Gynecol. 27, 422–431.

Donnez, J., Donnez, O., Matule, D., Ahrendt, H.J., Hudecek, R., Zatik, J., Kasilovskiene, Z., Dumitrascu, M.C., Fernandez, H., Barlow, D.H., Bouchard, P., Fauser, B.C., Bestel, E., Loumaye, E., 2016. Long-term medical management of uterine fibroids with ulipristal acetate. Fertil. Steril. 105, 165–173, e164.

Drosch, M., Schmidt, N., Markowski, D.N., Zollner, T.M., Koch, M., Bullerdiek, J., 2014. The CD24hi smooth muscle subpopulation is the predominant fraction in uterine fibroids. Mol. Hum. Reprod. 20, 664–676.

Dupasquier, S., Delmarcelle, A.S., Marbaix, E., Cosyns, J.P., Courtoy, P.J., Pierreux, C.E., 2014. Validation of housekeeping gene and impact on normalized gene expression in clear cell renal cell carcinoma: critical reassessment of YBX3/ZONAB/CSDA expression. BMC Mol. Biol. 15, 9.

Ishikawa, H., Ishi, K., Serna, V.A., Kakazu, R., Bulun, S.E., Kurita, T., 2010. Progesterone is essential for maintenance and growth of uterine leiomyoma. Endocrinology 151, 2433–2442.

Kampjarvi, K., Park, M.J., Mehine, M., Kim, N.H., Clark, A.D., Bützow, R., Böhling, T., Böhm, J., Mecklin, J.P., Järvinen, H., Tomlinson, I.P., van der Spuy, Z.M., Sjöberg, J., Boyer, T.G., Vahteristo, P., 2014. Mutations in Exon 1 highlight the role of MED12 in uterine leiomyomas. Hum. Mutat. 35, 1136–1141.

Kim, H., He, Y., Yang, I., Zeng, Y., Kim, Y., Seo, Y.W., Murnane, M.J., Jung, C., Lee, J.H., Min, J.J., Kwon, D.D., Kim, K.K., Lu, Q., Kim, K., 2012. delta-Catenin promotes E-cadherin processing and activates beta-catenin-mediated signaling: implications on human prostate cancer progression. Biochim. Biophys. Acta 1822, 509–521.

Kim, J.J., Sefton, E.C., 2012. The role of progesterone signaling in the pathogenesis of uterine leiomyoma. Mol. Cell. Endocrinol. 358, 223–231.

Leppert, P.C., Catherino, W.H., Segars, J.H., 2006. A new hypothesis about the origin of uterine fibroids based on gene expression profiling with microarrays. Am. J. Obstet. Gynecol. 195, 415–420.

Luyckx, M., Pirard, C., Fellah, L., Dereume, A., Mhallem, M., Debieve, F., Squifflet, J., 2016. Long-term nonsurgical control with ulipristal acetate of multiple uterine fibroids, enabling pregnancy. Am. J. Obstet. Gynecol. 214, 756, e1-2.

Malik, M., Segars, J., Catherino, W.H., 2012. Integrin beta1 regulates leiomyoma cytoskeletal integrity and growth. Matrix Biol. 31, 389–397.

McCall, M.N., McMurray, H.R., Land, H., Almudevar, A., 2014. On non-detects in qPCR data. Bioinformatics 30, 2310–2316.

Mehine, M., Kaasinen, E., Mäkinen, N., Katainen, R., Kämpjärvi, K., Pitkänen, E., Heinonen, H.R., Bützow, R., Kilpivaara, O., Kuosmanen, A., Ristolainen, H., Gentile, M., Sjöberg, J., Vahteristo, P., Aaltonen, L.A., 2013. Characterization of uterine leiomyomas by whole-genome sequencing. N. Engl. J. Med. 369, 43–53.

Mehine, M., Makinen, N., Heinonen, H.R., Aaltonen, L.A., Vahteristo, P., 2014. Genomics of uterine leiomyomas: insights from high-throughput sequencing. Fertil. Steril. 102, 621–629.

Mehine, M., Kaasinen, E., Heinonen, H.R., Mäkinen, N., Kämpjärvi, K., Sarvilinna, N., Aavikko, M., Vähärautio, A., Pasanen, A., Bützow, R., Heikinheimo, O., Sjöberg, J., Pitkänen, E., Vahteristo, P., Aaltonen, L.A., 2016. Integrated data analysis reveals uterine leiomyoma subtypes with distinct driver pathways and biomarkers. Proc. Natl. Acad. Sci. U.S.A. 113, 1315–1320.

Mittal, P., Shin, Y.H., Yatsenko, S.A., Castro, C.A., Surti, U., Rajkovic, A., 2015. Med12 gain-of-function mutation causes leiomyomas and genomic instability. J. Clin. Invest. 125, 3280–3284.

Nopparat, J., Zhang, J., Lu, J.P., Chen, Y.H., Zheng, D., Neufer, P.D., Fan, J.M., Hong, H., Boykin, C., Lu, Q., 2015. delta-Catenin, a Wnt/beta-catenin modulator, reveals inducible mutagenesis promoting cancer cell survival adaptation and metabolic reprogramming. Oncogene 34, 1542–1552.

Ono, M., Yin, P., Navarro, A., Moravek, M.B., Coon, J.S., 5th, Druschitz, S.A., Serna, V.A., Qiang, W., Brooks, D.C., Malpani, S.S., Ma, J., Ercan, C.M., Mittal, N., Monsivais, D., Dyson, M.T., Yemelyanov, A., Maruyama, T., Chakravarti, D., Kim, J.J., Kurita, T., Gottardi, C.J., Bulun, S.E., 2013. Paracrine activation of WNT/beta-catenin pathway in uterine leiomyoma stem cells promotes tumor growth. Proc. Natl. Acad. Sci. U.S.A. 110, 17053–17058.

Sandberg, A.A., 2005. Updates on the cytogenetics and molecular genetics of bone and soft tissue tumors: leiomyoma. Cancer Genet. Cytogenet. 158, 1–26.

Sasaki, H., Ohara, N., Xu, Q., Wang, J., DeManno, D.A., Chwalisz, K., Yoshida, S., Maruo, T., 2007. A novel selective progesterone receptor modulator asoprisnil activates tumor necrosis factor-related

apoptosis-inducing ligand (TRAIL)-mediated signaling pathway in cultured human uterine leiomyoma cells in the absence of comparable effects on myometrial cells. J. Clin. Endocrinol. Metab. 92, 616–623.

Selvais, C., Gaide Chevronnay, H.P., Lemoine, P., Dedieu, S., Henriet, P., Courtoy, P.J., Marbaix, E., Emonard, H., 2009. Metalloproteinase-dependent shedding of low-density lipoprotein receptor-related protein-1 ectodomain decreases endocytic clearance of endometrial matrix metalloproteinase-2 and -9 at menstruation. Endocrinology 150, 3792–3799.

Smyth, G.K., 2005. Limma: linear models for microarray data. In: Gentleman, R., Carey, V., Dudoit, S., Irizarry, R. (Eds.), Bioinformatics and Computational Biology Solutions using R and Bioconductor. Springer, New York, pp. 397–420.

Sternlicht, M.D., Werb, Z., 2001. How matrix metalloproteinases regulate cell behavior. Annu. Rev. Cell Dev. Biol. 17, 463–516.

Stewart, E.A., 2015. Clinical practice. Uterine fibroids. N. Engl. J. Med. 372, 1646–1655.

Tamm, K., Room, M., Salumets, A., Metsis, M., 2009. Genes targeted by the estrogen and progesterone receptors in the human endometrial cell lines HEC1A and RL95-2. Reprod. Biol. Endocrinol. 7, 150.

Tucker, R.P., Chiquet-Ehrismann, R., 2015. Tenascin-C: Its functions as an integrin ligand. Int. J. Biochem. Cell Biol. 65, 165–168.

Van Langendonckt, A., Romeu, L., Ambroise, J., Amorim, C., Bearzatto, B., Gala, J.L., Donnez, J., Dolmans, M.M., 2014. Gene expression in human ovarian tissue after xenografting. Mol. Hum. Reprod. 20, 514–525.

Vandesompele, J., De Preter, K., Pattyn, F., Poppe, B., Van Roy, N., De Paepe, A., Speleman, F., 2002. Accurate normalization of real-time quantitative RT-PCR data by geometric averaging of multiple internal control genes. Genome Biol. 3, RESEARCH0034.

Xu, Q., Takekida, S., Ohara, N., Chen, W., Sitruk-Ware, R., Johansson, E.D., Maruo, T., 2005. Progesterone receptor modulator CDB-2914 down-regulates proliferative cell nuclear antigen and Bcl-2 protein expression and up-regulates caspase-3 and poly(adenosine 5′-diphosphate-ribose) polymerase expression in cultured human uterineeiomyoma cells. J. Clin. Endocrinol. Metab. 90, 953–961.

Xu, Q., Ohara, N., Liu, J., Amano, M., Sitruk-Ware, R., Yoshida, S., Maruo, T., 2008. Progesterone receptor modulator CDB-2914 induces extracellular matrix metalloproteinase inducer in cultured human uterine leiomyoma cells. Mol. Hum. Reprod. 14, 181–191.

Yatsenko, S.A., Mittal, P., Wood-Trageser, M.A., Jones, M.W., Surti, U., Edwards, R.P., Sood, A.K., Rajkovic, A., 2017. Highly heterogeneous genomic landscape of uterine leiomyomas by whole exome sequencing and genome-wide arrays. Fertil. Steril. 107, 457–466, e459.

Yin, P., Roqueiro, D., Huang, L., Owen, J.K., Xie, A., Navarro, A., Monsivais, D., Coon, J.S., 5th, Kim, J.J., Dai, Y., Bulun, S.E., 2012. Genome-wide progesterone receptor binding: cell type-specific and shared mechanisms in T47D breast cancer cells and primary leiomyoma cells. PLoS ONE 7, e29021.

Yun, B.S., Seong, S.J., Cha, D.H., Kim, J.Y., Kim, M.L., Shim, J.Y., Park, J.E., 2015. Changes in proliferating and apoptotic markers of leiomyoma following treatment with a selective progesterone receptor modulator or gonadotropin-releasing hormone agonist. Eur. J. Obstet. Gynecol. Reprod. Biol. 191, 62–67.

Zeng, Y., Abdallah, A., Lu, J.P., Wang, T., Chen, Y.H., Terrian, D.M., Kim, K., Lu, Q., 2009. delta-Catenin promotes prostate cancer cell growth and progression by altering cell cycle and survival gene profiles. Mol. Cancer 8, 19.